https://doi.org/10.1016/j.vacuum.2018.04.028

Raman studies of MoS_2 under strain at different uniaxial directions

C.K.Tan, W.C.Wong, S.M.Ng, H.F.Wong, C.W.Leung, C.L.Mak

Department of Applied Physics, The Hong Kong Polytechnic University, Hung Hom, Hong Kong

E-mail address: apaclmak@polyu.edu.hk (C.L. Mak).

Highlights

- A modified bending technique has been employed to study the Raman spectra of MoS2 along different strain directions.

- The Raman shift rates of the quadrilayer MoS2 are sensitive to different applied strain directions.

- The armchair and zigzag directions of the exfoliated MoS2 might be determined by monitoring the variation of Raman shifts of the E12g and A1g modes in different strained directions.

Abstract

Raman spectra of bulk and few layers MoS_2 under strain at different uniaxial directions have been measured. MoS_2 samples, encapsulated in between polyethylene terephthalate (PET) of octadecagonal shape and a layer of polymethlmethacrylate (PMMA), were bended in order to apply uniaxial tensile strain along different directions of MoS_2. For bulk MoS_2, the Raman shift rates of the E^1_{2g} and A_{1g} modes (the change of the Raman peak position versus strain level) were very small and almost the same for strains applied along different directions. On the other hand, the Raman shift rates of few layers MoS_2 were larger than those in bulk MoS_2. In addition, they also exhibited distinctive anisotropic strain responses. On the basis of our results, we believe that the armchair and zigzag directions of the exfoliated MoS_2 might be determined by monitoring the variation of Raman shifts of the E^1_{2g} and A_{1g} modes in different strained directions of MoS_2.

Keywords

MoS_2, Strain effect and Raman response

1. Introduction

Strain engineering has been widely used for boosting the performance of optoelectronic, electronic and spintronic devices [1,2]. For example, the carrier mobility or the emission efficiency of light emitting devices can be enhanced by applying strain through bending of films on elastic substrates or inducing a lattice mismatch between films and substrates [1,3]. General speaking, the emerging 2D crystals such as MoS_2 are more suitable for strain engineering [4], as they have only one or few atoms in thickness. Therefore, few layers or monolayer MoS_2, have attracted great interests because of their distinctive electronic and optical properties; especially their band gap are highly sensitive to strain effect [5,6]. Recently, Hui et al. measured the Raman spectra of compressively strained tri-layer MoS_2 sheet on top of a piezoelectric actuator substrate [7]. For an applied strain of 0.2%, the two feature peaks at 380 cm^{-1} and 400 cm^{-1} shifted by ∼3 and ∼2 cm^{-1}, respectively [7]. He et al. studied the strain dependency of optical absorption and photoluminescence of atomically thin MoS_2 deposited on top of PMMA [8]. They reported that under relatively small strains, a redshift of ∼70 meV/% strain was observed for the direct-gap exciton for both mono- and bi-layer MoS_2 [8]. Furthermore, the effects of strain on the properties of chemical vapour deposition (CVD) grown monolayer MoS_2 have been extensively studied for recent years [9]. These studies have demonstrated that monolayer MoS_2 can be very useful for the development of optoelectronic devices. So far, limited research has been reported on the effects of strain along different MoS_2 directions on exfoliated MoS_2. In this paper, we demonstrate a modified bending technique to apply uniaxial tensile strain along different directions of MoS_2 and report their corresponding Raman spectra. On the basis of our measurements, we believe that the armchair and zigzag directions of exfoliated MoS_2 can be determined by monitoring the variation of Raman shift in different strained directions.

2. Experimental methods

Polyethylene terephthalate (PET), a transparent and conventional plastic, was used as substrate for this experiment. Firstly, the PET sheet with thickness of ~0.12 mm was cut into an octadecagon shape with 24 mm in diameter. The octadecagon PET was then spin-coated with SU-8 photoresist (≈400 nm) at a speed of 4000 rpm for 40 s to enhance the visibility of MoS_2 and reduce the surface roughness of the PET. In addition, the SU-8 layer served as a buffer layer to increase the adhesion between MoS_2 and PET [10,11]. The SU-8 coated PET sheets were then baked at 110 °C for 10 min to evaporate the excess solvent of SU-8. Then mechanically exfoliated MoS_2 was deposited at the centre of the PET substrate. As the size of the transferred MoS_2 samples (~several μm in size) were very small compared to the thickness of PET substrate, therefore the induced strain to the flakes can be assumed to be the same as the applied strain to the PET substrate [12]. Finally, a thin layer of Poly(methylmethacrylate) (PMMA) of thickness around 100 nm was immediately spin-coated on top of the deposited MoS_2 using a spin-coater operated at 4000 rpm for 30s. The PMMA layer was used to prevent the slipping and protect the MoS_2 from degradation in ambient. The sample was then baked at 110 °C for 1 min to harden the PMMA layer. As the baking temperature is relatively low, we believe that no strain orientation is existed in the MoS_2 layer. 3D printer was used to build rectangular moulds of different sizes as shown in Fig. 1. The samples were mounted inside the moulds with different sizes. Through mounting the PET substrates in different moulds, the PET substrates were bended differently at different strain levels. As a result, strains from 1% up to 8% were induced to the PET substrate.

PET substrate was mounted inside the 3D mould, and the sample sitting on PET substrate was measured by Raman spectroscopy. Raman spectra were measured using a 488 nm laser line of an air cooled Ar-ion laser. A microscope was used to focus the incident laser beam to a spot of about 2 µm in diameter. The Raman spectra were recorded by a 100x lens system in backscattering geometry using a Horiba-JobinYvon HR800 spectrometer equipped with a charge-coupled device detector. Here, as the MoS_2 is very thin so the laser in the Raman system should penetrate the samples. Six Raman spectra were obtained for each strain level and an average Raman shift for each peak was calculated. After taking the Raman spectra under the specific uniaxial strain, PET substrate was removed from the 3D mould to fully release its strain for one day. In the next day, the PET substrate was mounted in the same 3D mould with the same applied uniaxial strain level but with a 20° rotation with respect to previous measurement. Thus, the procedures were repeated so that Raman spectra of 0° rotation (referred to the orientation at the first measurement) upto 180° rotation were measured. Afterwards, the measurements were repeated using different 3D moulds under different strain levels (upto 8% strain). Finally, the Raman spectra for encapsulated MoS_2 of different thicknesses were also studied to compare the respond of different samples.

3. Results and discussion

A typical Raman spectrum of encapsulated quadrilayer MoS_2 on PET substrate without applied uniaxial strain is shown in Fig. 2. Lorentzian peak fitting was employed to obtain the peak position of the measured E2g1 and A_{1g} modes of MoS_2. The obtained Raman peak separation was 24 cm^{-1} which is corresponding to quadrilayer MoS_2 reported in the literature [13]. For the bulk MoS_2, Raman separation of the feature peaks was roughly 25 cm^{-1} which was similar to the reported value [13].

Raman shifts of E2g1 and A_{1g} modes of the quadrilayer MoS_2 in the uniaxial strain direction of 60° orientation as a function of applied strain level is shown in Fig. 3. General speaking, as the strain level increased, the intensities and the shape of the peaks remained roughly the same, but their peak positions shifted to different values, i. e both the E2g1 and A_{1g} modes were red shifted in most case. The blue and the red lines in the figure are the least-square-fitting for the data, and the slope of the fits was noticed to be the Raman shift rate. Table 1 summarizes the Raman shift rates of the two vibrational modes of the bulk and 4-layer MoS_2 for different uniaxial strain directions. Positive sign in the table indicates blue shift of the vibrational mode and negative sign means red shift. For E2g1 mode in bulk MoS_2, Raman shift rates greater than 0.5 cm^{-1}/% strain were observed in applied uniaxial strain directions from 0° to 80°. Raman shift rate E2g1 had the biggest value when the uniaxial strains were applied along 0° and 40°. On the other hand, for A_{1g} mode, the largest value was observed at strain direction of 40°. Most of the directions in A_{1g} mode had Raman shift rates smaller than 0.5 cm^{-1}. Indeed, some of the changes were small and might be within the limitation of the system resolution.

For quadrilayer MoS_2 in different applied uniaxial strain, the Raman shift rates were in general larger than those in bulk sample. Most of the Raman shift rate for A_{1g} mode had values higher than 0.5 cm^{-1}/% strain especially in the direction of 60°. Similarly, most of the Raman shift rates for E2g1 mode were larger than 0.5 cm^{-1}/% strain and the highest value was at the direction of 60°. Similar trend was also observed in A_{1g} mode. Both modes have a red shift rate that around 1.5 at 60° orientation. When a further 60° is applied onto it, which is around 120°, both modes became very insensitive to the applied uniaxial strain i.e. the Raman shift rate was relatively small. This observation might indicate that applied uniaxial strain at 60° is relative to the armchair direction of quadrilayer MoS_2. This might explain why in this direction it has a very high Raman shift rate for both modes. Furthermore, when a further 60 °angle was applied, the uniaxial strain has attributed along the zigzag direction, which might explain that the Raman shift rate becomes relatively not sensitive to the applied uniaxial strain. It has also been reported that the anisotropic thermoelectric behavior in armchair and zigzag directions can behave differently [12]. Therefore, we believe that the different Raman shift rates in armchair and zigzag direction can be used as a method to determine the crystalline orientation direction of exfoliated samples.

4. Conclusion

In summary, comprehensive study of the anisotropic strain response in Raman modes of different thicknesses MoS_2 using a modified bending technique has been carried out. The Raman shift rates of the E2g1 and A_{1g} modes of the bulk MoS_2, are not sensitive to different applied strain directions. On the other hand, when the applied strain direction applied to the quadrilayer MoS_2 was 60° with respect to the original direction, it had the highest Raman shift rate among the others for both E2g1 and A_{1g} modes. When an additional 60 ^{o}was added i.e. crystalline direction changes from armchair to zigzag direction, Raman shift rate became very small. Based on the anisotropic strain response in E2g1 and A_{1g} modes for mono or few layer MoS_2, this work shows the possibility of a simply method to identify the crystalline orientation of thin MoS_2 using the strained exfoliated MoS_2 and the Raman spectroscopy. The modified bending technique in this work can also be used to investigate other electrical, optical or thermal property of other 2D materials which can bring a significant influence in fabrication of devices.

Acknowledgements

This work was supported by a research grant of The Hong Kong Polytechnic University (PolyU GUA5G). C. K. Tan was supported by a MPhil studentship of the Hong Kong Polytechnic University.

Fig. 1. 3D moulds built by 3D printer with different sizes.

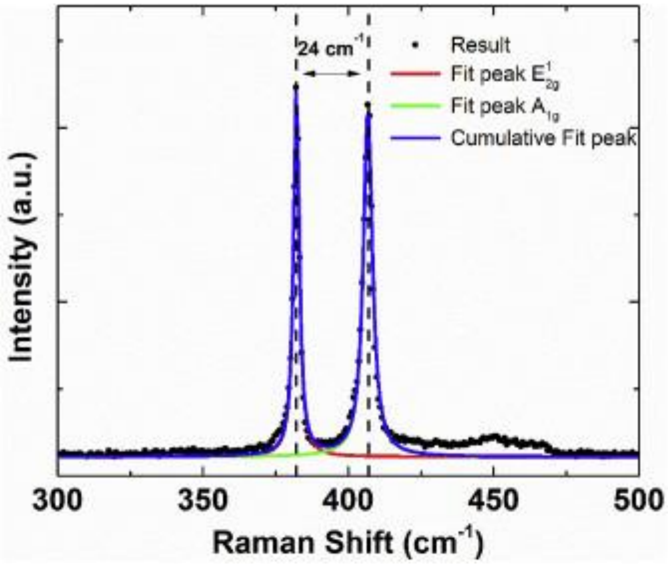

Fig. 2. Raman spectra of the encapsulated quadrilayer MoS_2 on PET substrate without applied uniaxial strain.

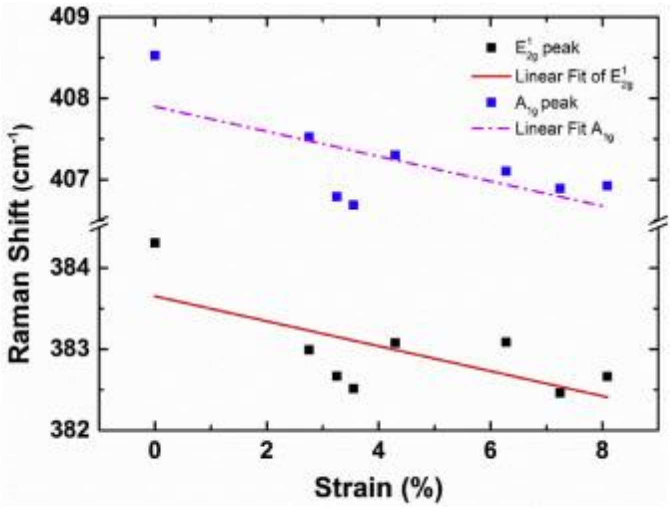

Fig. 3. Raman shift of E2g1 and A_{1g} modes of the quadrilayer MoS_2 in the uniaxial strain direction in 60° together with linear fitting.

Table 1. Raman shift rate of E2g1 and A_{1g} modes of the bulk and 4-layer MoS_2 for different uniaxial strain directions respectively.

Direction/degree	**Raman Shift rate (cm^{-1}/Strain)**			
	Bulk	**Bulk**	**4-layer**	**4-layer**
	E2g1	$\mathbf{A_{1g}}$	E2g1	$\mathbf{A_{1g}}$
160	−0.31	−0.22	−0.60	−0.13
140	−0.43	−0.13	−0.89	−0.64
120	−0.25	0.11	0.15	0.38
100	0.18	0.17	−0.31	0.32
80	−0.54	−0.31	−1.00	−0.30
60	−0.7	−0.07	−1.54	−1.53
40	−1.19	−0.47	−0.86	−1.03
20	−0.67	−0.11	−0.52	−0.43
0	−1.20	−0.16	−0.13	−0.21

References

[1] Y. Kato, R.C. Myers, A.C. Gossard, D.D. Awschalom, Coherent spin manipulation without magnetic fields in strained semiconductors, Nature 427 (6969) (2004) 50–53.

[2] X. Xu, W. Yao, D. Xiao, T.F. Heinz, Spin and pseudospins in layered transition metal dichalcogenides, Nat. Phys. 10 (5) (2014) 343–350.

[3] C. Pan, L. Dong, G. Zhu, S. Niu, R. Yu, Q. Yang, Y. Liu, Z.L. Wang, High-resolution electroluminescent imaging of pressure distribution using a piezoelectric nanowire LED array, Nat. Photon. 7 (9) (2013) 752–758.

[4] C. Lee, X. Wei, J.W. Kysar, J. Hone, Measurement of the elastic properties and intrinsic strength of monolayer graphene, Science 321 (5887) (2008) 385–388.

[5] P. Lu, X. Wu, W. Guo, X.C. Zeng, Strain-dependent electronic and magnetic properties of MoS2 monolayer, bilayer, nanoribbons and nanotubes, Phys. Chem. Chem. Phys. 14 (37) (2012) 13035–13040.

[6] Q.H. Wang, K. Kalantar-Zadeh, A. Kis, J.N. Coleman, M.S. Strano, Electronics and optoelectronics of two-dimensional transition metal dichalcogenides, Nat. Nanotechnol. 7 (11) (2012) 699–712.

[7] Y.Y. Hui, X. Liu, W. Jie, N.Y. Chan, J. Hao, Y.-T. Hsu, L.-J. Li, W. Guo, S.P. Lau, Exceptional tunability of band energy in a compressively strained trilayer MoS2 sheet, ACS Nano 7 (8) (2013) 7126–7131.

[8] K. He, C. Poole, K.F. Mak, J. Shan, Experimental demonstration of continuous electronic structure tuning via strain in atomically thin MoS2, Nano Lett. 13 (6) (2013) 2931–2936.

[9] A. Castellanos-Gomez, R. Roldán, E. Cappelluti, M. Buscema, F. Guinea, H.S.J. van der Zant, G.A. Steele, Local strain engineering in atomically thin MoS2, Nano Lett. 13 (11) (2013) 5361–5366.

[10] G. Tsoukleri, J. Parthenios, K. Papagelis, R. Jalil, A.C. Ferrari, A.K. Geim, K.S. Novoselov, C. Galiotis, Subjecting a graphene monolayer to tension and compression, Small 5 (21) (2009) 2397–2402.

[11] C. Casiraghi, A. Hartschuh, E. Lidorikis, H. Qian, H. Harutyunyan, T. Gokus, K.S. Novoselov, A.C. Ferrari, Rayleigh imaging of graphene and graphene layers, Nano Lett. 7 (9) (2007) 2711–2717.

[12] C. Rice, R.J. Young, R. Zan, U. Bangert, D. Wolverson, T. Georgiou, R. Jalil, K.S. Novoselov, Raman-scattering measurements and first-principles calculations of strain-induced phonon shifts in monolayer MoS${ }_{2}$, Phys. Rev. B 87 (8) (2013) 081307.

[13] H. Li, Q. Zhang, C.C.R. Yap, B.K. Tay, T.H.T. Edwin, A. Olivier, D. Baillargeat, From bulk to monolayer MoS2: evolution of Raman scattering, Adv. Funct. Mater. 22 (7) (2012) 1385–1390.